Effect of oxygen non-stoichiometry on the electrochemical performance of lithium manganese oxide spinels

A.R. Naghash, Jim Y. Lee[*]

Department of Chemical and Environmental Engineering, National University of Singapore, 10 Kent Ridge Crescent, Singapore 119260, Singapore

Abstract

The effect of oxygen non-stoichiometry on the electrochemical performance of lithium manganese oxide spinels is investigated. Spinels with different oxygen contents are obtained from citrate gel synthesis followed by calcination in air in the temperature range 200–850°C. Spinels that were formed at low temperatures are found suitable for 3 V applications, whereas those formed at high temperatures perform better at 4 V. Both type of spinels cycle well in their respective potential regimes. © 2001 Elsevier Science B.V. All rights reserved.

1. Introduction

Lithium manganese oxide spinel as a 4 V cathode material has been investigated since the early 1980s [1–7]. The material is currently synthesized by solid-state reactions, using MnO_2 along with either Li_2CO_3 or $LiNO_3$ as the starting materials and at temperatures around 800°C. Heating of $MnCO_3$ and Li_2CO_3 at 400°C produces $Li_2Mn_4O_9$ and $Li_4Mn_5O_{12}$ spinels which are more suited for 3 V applications [8,9]. For good 3 V capacities, it is important to obtain spinels with as high a Mn^{4+} concentration as possible (e.g. $Li_2Mn_4O_9$ and $Li_4Mn_5O_{12}$) [10]. Stoichiometric $LiMn_2O_4$ from high-temperature reactions is a 50:50 mixture of Mn^{3+} and Mn^{4+}, and hence, does not perform well at the 3 V plateau. For the same reason, oxygen-rich spinels ($LiMn_2O_{4+x}$) in which the Mn^{4+} cations outnumber the Mn^{3+} by four times per mole of spinel should be more functional at 3 V than at 4 V. Table 1 shows the capacities of oxygen-rich spinels with different x-values. It is known that as the synthesis temperature is decreased, the x-value increases [10]. Oxygen-rich spinels should therefore be prepared at low temperatures; high-temperature, solid-state reactions are not suitable routes. The citrate gel synthesis, or the more elaborate Pechini process, is a good low-temperature method. Han and Kim [11] investigated the effect of ethylene glycol (EG) in synthesis on the physical and electrochemical properties of the spinel. They suggested

the use of excess lithium to compensate for lithium evaporation during the pre-ignition of metals–citrate complexes. On the other hand, Choy et al. [12] investigated the effect of sintering temperature and atmosphere on the physicochemical properties of the $LiMn_2O_4$ spinel [12].

In comparison to previous studies, this work aims to (i) develop a new heat-treatment procedure to reduce the loss of lithium through evaporation during synthesis; (ii) vary the heat-treatment to produce spinels optimized for 3 and 4 V applications, respectively. Citric acid chelation of the metal ions is again chosen the basis of the sol formation in aqueous solutions. The cations in the chelates are mixed at the atomic scale, which thereby allows lower temperatures to be used for the heat-treatment.

2. Experimental procedure

2.1. Citrate gel synthesis of lithium manganese spinels

Citric acid monohydrate (Merck, 99.5%), $LiNO_3$ (Sigma, 99%), and $Mn(NO_3)_2$ (Fluka, 97%) were of the purest grade commercially available and used as received. The sol–gel synthesis began by mixing Li and Mn salts in the atomic ratio of Li:Mn = 0.5 with citric acid according to citric acid:(Li + Mn) = 1. For a specific example, 0.05 mol $LiNO_3$ (3.45 g) and 0.1 mol $Mn(NO_3)_2$ (17.9 g) were mixed in 300 ml of distilled water with continuous stirring at room temperature. An amount of 0.15 mol citric acid in distilled water was added to the mixed metal solution. The clear

* Corresponding author. Tel.: +65-874-2899; fax: +65-779-1936.
E-mail address: cheleejy@nus.edu.sg (J.Y. Lee).

Table 1
Capacity of $LiMn_2O_{4+x}$ for different x-values

x	Theoretical 3 V capacity (mAh g^{-1})	Theoretical 4 V capacity (mAh g^{-1})
0	148	148
0.02	156	140
0.06	165	130
0.08	170	124
0.10	176	118

solution turned to a sol when the pH was adjusted to 6 using dilute aqueous ammonia while stirring continued overnight at room temperature. The rapid removal of the solvent in a rotary evaporator under vacuum at 70°C prevented the re-crystallization of the lithium–manganese–citrate complex. The vitreous precursor so obtained was a semi-dried paste with a glossy and slightly pinkish appearance. The precursor was dried in a oven below 100°C overnight before it was heated to various temperatures between 200 and 850°C to form the spinels. For the convenience of representation, the code Sxxx is used to denote a spinel prepared at temperature xxx, e.g. spinel prepared at 650°C is denoted by S650.

2.2. Materials characterizations

X-ray diffraction analyses of $LiMn_2O_4$ and various inter-mediate oxides were carried out on a Shimadzu XRD-6000 automated X-ray powder diffractometer using monochro-mated Cu Kα radiation ($\lambda = 1.542$ Å). Elemental analysis was by means of inductively-coupled plasma spectroscopy (ICPS) on a Perkin-Elmer Optima 3000 using aqua regia digestion of the spinels. In order to determine the Mn oxidation state in the spinels, a chemical analysis based on a sequence of redox titrations involving MnO_4^-/Mn^{2+}, Mn^{3+}/Mn^{2+}, and Fe^{3+}/Fe^{2+} couples was used [13]. A Philips XL 30 scanning electron microscope allowed exam-ination of spinel morphology.

2.3. Electrochemical characterization

Electrochemical characterization of the spinels was car-ried out in two-electrode test cells with metallic lithium counter electrodes, as described in our previous work [14]. The positive electrode was constituted from a slurry of 87 wt.% spinel, 6 wt.% carbon black and 7 wt.% PVDF in N-methylpyrrolidon (NMP). The electrode mixture was pasted onto an Al foil and dried at 50°C overnight. Cylind-rical cathode pellets were punched from the foil and com-pressed at 1–2 T cm^{-2} before further drying at 120°C for 12 h. A commercial (Merck) 1 M LiPF$_6$ solution in 1:1 (w/w) EC/DMC mixture served as the electrolyte. The test cells were galvanostatically cycled between the potential limits of 4.5 and 3 V for the 4 V plateau, and 3.7 and 2 V for the 3 V plateau, on a Maccor series 2000 battery life cycle tester at 0.2 mA cm^{-2}.

3. Results and discussion

3.1. Physical characterizations

3.1.1. X-ray diffraction patterns

Han and Kim [11] reported that in the absence of ethylene glycol (EG), the auto-ignition of the oxide precursor in air and the subsequent calcination results in spinels of low lithium content and Mn_2O_3 as the impurity phase. We have noted a rapid increase in the heat-treatment temperature is another contributing factor. Lithium evaporation is therefore caused by high local temperatures in the complex char (>900°C) in the auto-ignition of the precursor [11]. For this reason, an improved heat-treatment procedure has been used to prepare spinels from the metals–citrate complex. The metal complex is heated at 1°C min^{-1} to 180°C and soaked at 180°C for 24 h. A puffed char is obtained when the temperature reaches 180°C. The temperature is then raised to 200°C and kept at this temperature for 3 days. The step-wise process allows a slow decomposition of the precursor so that lithium evaporation due to rapid increase in the temperature is prevented during synthesis.

From the XRD patterns of oxide precursors heat-treated at different temperatures, the spinel structure is detected after prolonged heating (3 days) at 200°C (Fig. 1). Despite the extremely low reaction temperature and without using EG, there is no evidence of any peak from phases other than the spinel. Multiple phases have often been detected in spinel synthesis without EG even at 600°C [11]. All the peaks in the XRD patterns can be indexed by $LiMn_2O_4$. Fig. 2 shows the lattice parameter a of the spinels as a function of the heat-treatment temperature. The lattice parameter is 8.19 Å for the spinel prepared at 200°C for 3 days, which is slightly
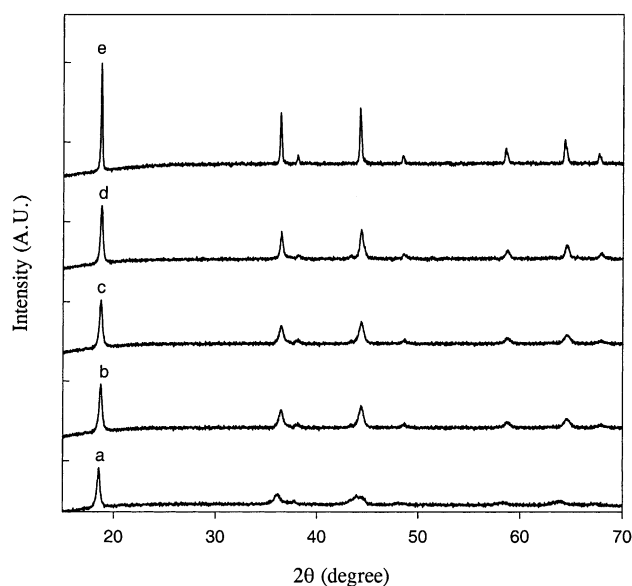

Fig. 1. XRD patterns of oxide precursors heat treated at (a) 200°C for 100 h, (b) 350°C for 48 h, (c) 450°C for 48 h, (d) 650°C for 48 h and (e) 850°C for 3 h.
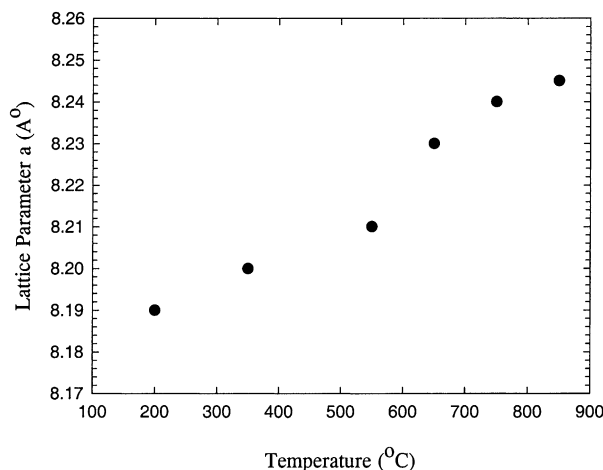
Fig. 2. Lattice parameter *a* of spinels prepared at different temperatures.

Table 2
Composition of $LiMn_2O_{4+x}$ spinels prepared at different temperatures

Sample	Li:Mn from ICPS	$\bar{x}$ from redox titrations	Average Mn valency
S200	0.99:2	0.12	3.62
S350	0.99:2	0.09	3.59
S550	0.98:2	0.05	3.55
S650	0.98:2	0.02	3.52
S750	0.99:2	0	3.5
S850	0.99:2	0	3.5

the starting materials is able to reduce particle sintering in the solid-state preparation of oxides at higher temperatures. It should be emphasized that all carbon residuals will eventually leave the system as gases.

3.1.2. Elemental composition

The results from redox titrations, together with the ICPS determinations of the metal contents, are summarized in Table 2. The Li:Mn ratios of the spinels are evidently not compromised by the sol–gel preparation, and the stoichiometry of Li:Mn = 1:2 in the starting mixtures is largely preserved, even though no excess lithium is used. The presence of oxygen-rich compositions, and hence average Mn oxidation states greater than +3.5, is an expected outcome of low-temperature preparations.

3.2. Electrochemical characterizations

3.2.1. Cyclic voltammetry

The cyclic voltammograms of S200, S450, S650 and S850 spinels are shown in Fig. 4. The potential was swept between 2 and 4.5 V at a scan rate of 3 mV min^{-1} for one cycle. All
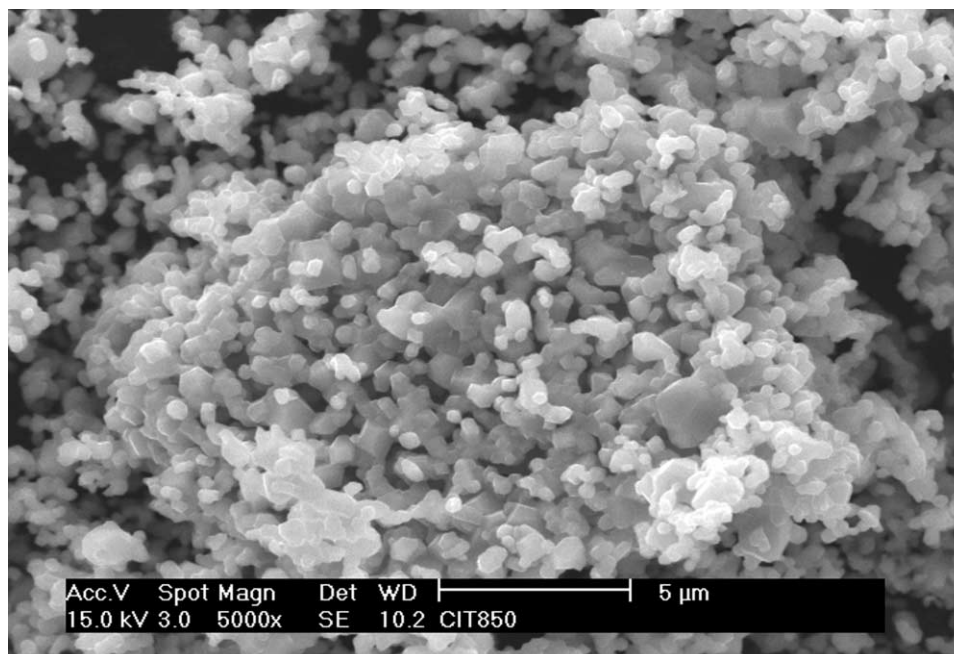
refined ('increased') with increase in temperature (from 8.190 Å at 200°C to 8.245 Å at 850°C). This result is consequential upon the presence of well-mixed precursors to reduce the diffusion barrier in the resulting solid-state reactions, so that lower temperatures can be used.

A scanning electron micrograph of a spinel prepared at 850°C for 3 h is presented in Fig. 3. It clearly indicates a particle size in the sub-micron range. The good morphology can be attributed to two main factors: (i) the formation of spinel at low temperatures around 200°C; (ii) the use of organic precursors. When the organic precursors are decomposed to carbon and carbon derivatives, the decomposed products can serve as spacers between the particles to prevent the sintering of the latter at high temperatures. It has been reported [15] that a small amount of carbon in

Fig. 3. SEM image of spinel prepared at 850°C for 3 h.
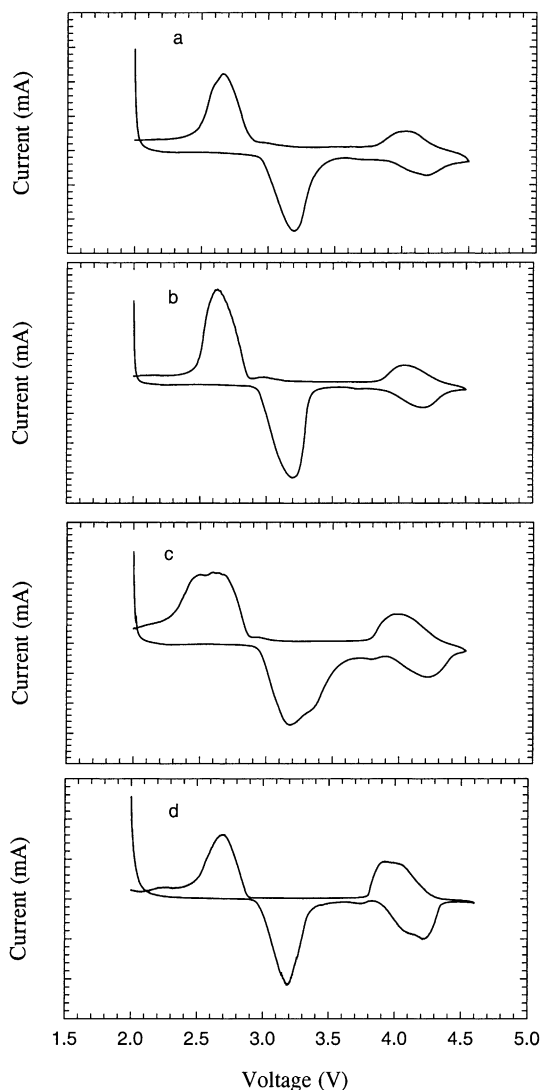
Fig. 4. Cyclic voltammograms of (a) S200, (b) S450, (c) S650 and (d) S850.

Table 3
Theoretical, expected[a], and measured capacities (0.2 mA cm^{-2}) of LiMn$_2$O$_{4+x}$ spinels heat treated at different temperatures (4 V applications)

Sample	x	Theoretical capacity (mAh g^{-1})	Expected[a] capacity (mAh g^{-1})	Measured capacity (mAh g^{-1})
S200	0.12	110	88	70
S350	0.09	120	96	82
S550	0.05	133	107	80
S650	0.02	140	112	105
S750	0	148	119	110
S850	0	148	119	118

[a] As 80% of theoretical.

voltammograms show the two characteristic redox pairs expected for a LiMn$_2$O$_4$ spinel: one between 3.5 and 4.5 V, the other between 2 and 3.5 V. These correspond, respectively, to the first and second Li$^+$ intercalation and de-intercalation reactions with the spinel host. Furthermore, the spinel formed at the lowest temperature (200°C) is electrochemically similar to that formed at the highest temperature (850°C). The low-temperature spinel (Fig. 4(a)) is able to deliver a more reversible charge in the lower potential region. Increase in the calcination temperature increases only the reversible charge in the upper potential region (3.5–4.5 V). This is consistent with the predominance of the 4 V plateau in high-temperature spinels.

3.2.2. Capacities for the 4 V plateau

The theoretical and measured capacities of oxygen-rich spinels from the citrate process are listed in Table 3. High heat-treatment temperatures result in less-oxidized spinels with decreasing x in the composition LiMn$_2$O$_{4+x}$. As

expected, the capacities for the 4 V plateau increase with the heat-treatment temperature as the stoichiometry approaches that of LiMn$_2$O$_4$. A plot of measured capacity against calcination temperature is given in Fig. 5. A discharge capacity of 70 mAh g^{-1} is obtained from the S200 spinel. The capacity does not increase significantly until the temperature is at least 450°C, and beyond 650°C the capacity is again almost temperature invariant. A maximum capacity of 118 mAh g^{-1} is obtained after heat-treatment at 850°C for 3 h. Since, the S750 and S850 spinels both have the same composition ($x = 0$), the increase in capacity of the latter could be attributed to its improved crystallinity. The large difference between the expected and measured capacities in low-temperature spinels is also likely the result of poor crystallinity. Increase in the heat-treatment temperature can bring about refinements in both the stoichiometry and crystallinity. By increasing the temperature from 750 to 850°C, and by reducing the heating time from 24 to 3 h, a 8% increase in capacity is possible. This indicates the overriding influence of temperature over heating time, especially at higher temperatures. An unduly high temperature is, however, counter-productive as it may cause spinel decomposition. Experimentally, the spinel prepared at 850°C for 3 h offers the best performance in terms of realizable capacity.

The charge and discharge curves of S850 between the potential limits of 3.5 and 4.5 V at a current density of 0.2 mA cm^{-2} are given in Fig. 6. The cell was discharged immediately upon completion of charge. The slight increase in the second cycle performance is due to cathode conditioning. Lithium de-intercalation in the second cycle consumed 126 mAh g^{-1}, and the composition of the spinel after charging to 4.5 V was Li$_{0.14}$Mn$_2$O$_4$ with 0.86 mole of Li ions extracted per formula unit. The reverse process returned 122 mAh g^{-1} of charge, which corresponds to a coulombic efficiency of 96%. Therefore, it can be concluded that only 80% of the theoretical capacity can be utilized reversibly, as is expected for most spinel cathodes.

Variations in the capacity of the S850 cathode upon cycling are shown in Fig. 7. It is immediately evident that this material offered a very substantial improvement in cycleability over spinels prepared by other methods
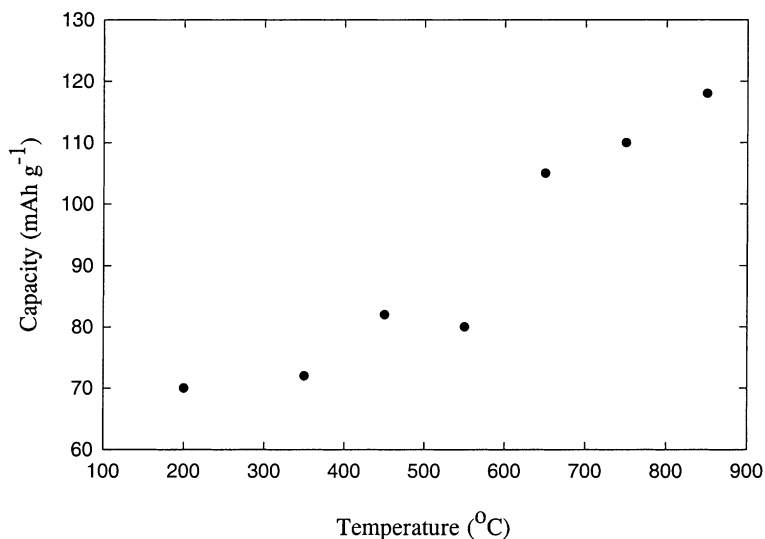
Fig. 5. Initial discharge capacities of $LiMn_2O_{4+x}$ as a function of calcination temperature.

[11,12]. After a brief conditioning period in the first few cycles, the capacity stabilizes to $119\,\mathrm{mAh\,g^{-1}}$ with no noticeable capacity fading in 50 cycles.

3.2.3. Capacities for the 3 V plateau

It was shown in Table 1 that the capacities of spinels at 3 V increase with increasing x in $LiMn_2O_{4+x}$ (or decreasing calcinations temperature). This can be explained in terms of a higher ratio of Mn^{4+} to Mn^{3+} in the low-temperature spinels. Although S200 does not perform well in the 4 V plateau because of its low practical capacity ($70\,\mathrm{mAh\,g^{-1}}$), it cycles rather well at 3 V. The cycleability of S200, S350, S550, S650 and S850 spinels between 2 and 3.7 V at a current density of $0.2\,\mathrm{mA\,cm^{-2}}$ for 20 cycles is shown in Fig. 8. For S200, a discharge capacity of $162\,\mathrm{mAh\,g^{-1}}$ is

obtained from the first cycle. After 20 cycles, 17% of the initial discharge capacity is lost. For S350, the first cycle discharge capacity is $151\,\mathrm{mAh\,g^{-1}}$ and 20% of this is lost in 20 cycles. As the calcination temperature is increased further, the cycling performance becomes poorer (e.g. 31% loss of initial discharge capacity for S850 after 20 cycles). This is in stark contrast with the behavior of these materials at 4 V. If it is believed that temperature affects crystallinity, then a less-crystalline material is more suited for 3 V applications, whereas a highly crystalline spinel is more suited for 4 V applications.

As low temperatures lithium manganese spinels have four times less moles of high-spin Mn^{3+} cations in the structure (relative to stoichiometric $LiMn_2O_4$), less octaherdrons are distorted due to Jahn–Teller effects. The distortion causes a
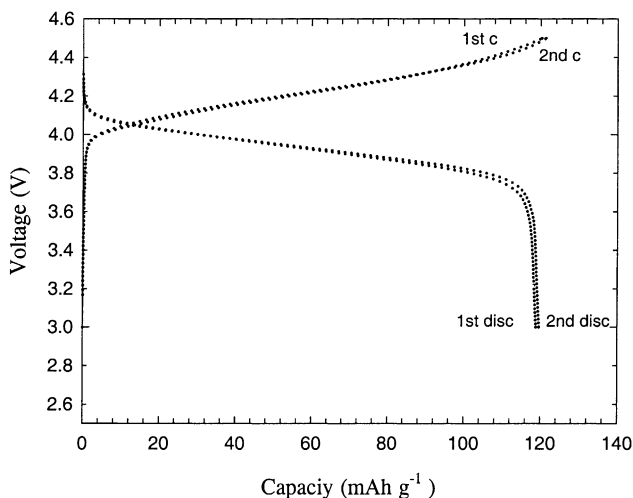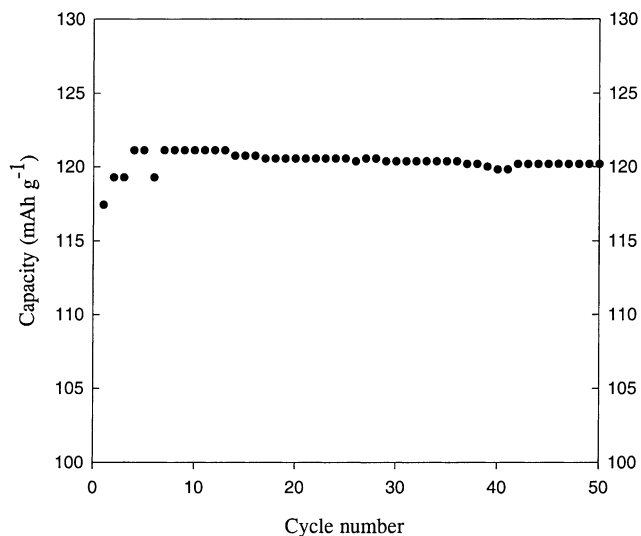

Fig. 6. Charge and discharge curves of S850.
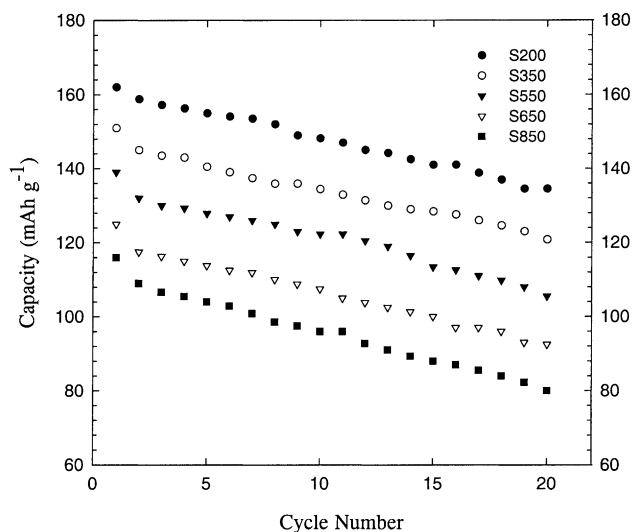

Fig. 7. Cycleability of S850.

Fig. 8. Cycleability of spinels in potential range of 2–3.7 V and at current density of 0.2 mA cm^{-2} for 20 cycles: (●) S200; (○) S350; (▼) S550; (▽) S650; (■) S850.
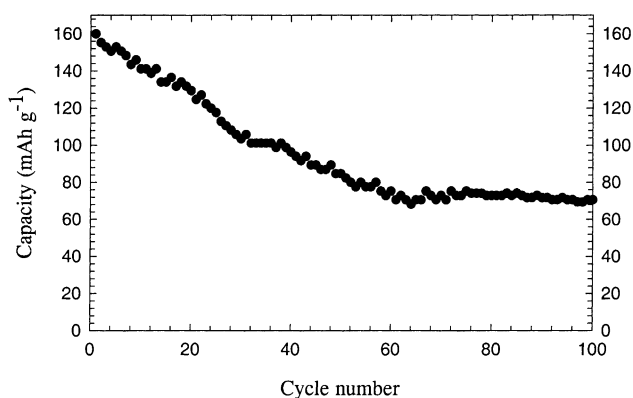

Fig. 9. Cycleability of S200 between 2 and 3.7 V at 0.2 mA cm^{-2}.

cubic to tetragonal phase transition which severely affects the cycling performance at 3 V. The higher tolerance of the low-temperature spinels on cycling can, therefore, be attributed in part to a lower amount (four times less moles) of high-spin Mn^{3+} cations in the structure. The cycling performance of S200 at a current density of 0.2 mA cm^{-2} for 100 cycles is shown in Fig. 9. This material lost only 50% of its initial capacity after 100 cycles. This is a very good performance for a 3 V spinel.

4. Conclusions

Lithium manganese oxide spinels have been obtained from a sol–gel process. Based on this method, spinels with varying oxygen contents are obtained as a function of the calcination temperature. Phase-pure spinel with the formula LiMn$_2$O$_{4.12}$ can be formed at temperatures as low as 200°C after 100 h of heating. Increase in the calcination temperature brings the composition closer to stoichiometric LiMn$_2$O$_4$. At 750°C, a composition very close to LiMn$_2$O$_4$ is possible. Good product crystallinity can only be obtained, however, by increasing the temperature to 850°C for a short period of time (3 h). In terms of capacity, the low-temperature spinels have lower capacities for the 4 V plateau because of a smaller proportion of Mn^{3+} cations in their structures. By contrast, capacities for the 3 V plateau are correspondingly higher because of their higher Mn^{4+} concentrations. A more crystalline spinel is beneficial to good performance at the 4 V plateau, but inconsequential or even detrimental to the 3 V performance. In a low-temperature spinel, less octahedrons are distorted by Jahn–Teller effects because of fewer Mn^{3+} cations compared with Mn^{4+} cations.

References

[1] J.M. Tarascon, W.R. Mckinnon, F. Coowar, T.N. Bowner, G. Amatucci, D. Guyomard, J. Electrochem. Soc. 141 (1994) 1421.
[2] J.M. Tarascon, D. Guyamard, Solid State Ionics 69 (1994) 293.
[3] J.M. Tarascon, F. Wang, F.K. Shokoohi, W.R. Mckinnon, D. Colsan, Electrochem. Soc. 138 (1991) 2859.
[4] J.M. Tarascon, F. Coowar, G. Amatici, F.K. Shokoohi, D.G. Guyomard, J. Power Sources 54 (1995) 103.
[5] M.M. Thacheray, J. Electrochem. Soc. 142 (1995) 2558.
[6] G. Pistoia, R. Rosati, J. Power Sources 58 (1996) 135.
[7] D. Guyomard, J.M. Tarascon, Solid State Ionics 69 (1994) 222.
[8] T. Nohma, Y. Yamamoto, I. Nakane, N. Furukawa, J. Power Sources 32 (1990) 373.
[9] M.M. Thackeray, A. de Kock, M.H. Rossouw, D. Liles, R. Bittihn, D. Hoge, J. Electrochem. Soc. 139 (1992) 363.
[10] M.M. Thackeray, M.H. Rossouw, A. de Kock, A.P. de la harpe, R.J. Gummouw, K. Pearce, D.C. Liles, J. Power Sources 43/44 (1993) 289.
[11] Y.-S. Han, H.-G. Kim, J. Power Sources 88 (2000) 161.
[12] J.-H. Choy, D.-H. Kim, C.-W. Kwon, S.-J. Hwang, Y.-I. Kim, J. Power Sources 77 (1999) 1.
[13] K.J. Vetter, N. Jeager, Electrochim. Acta 11 (1966) 401.
[14] A.R. Naghash, J.Y. Lee, J. Power Sources 85 (2000) 284.
[15] M. Ekelund, B. Forslund, J. Am. Ceram. Soc. 75 (1992) 532.